Letter

Crystal Structure of Sphingosine Kinase 1 with PF-543

Jing Wang,[†] Stefan Knapp,[†,‡] Nigel J. Pyne,[§] Susan Pyne,[§] and Jonathan M. Elkins*,[†]

[†]Structural Genomics Consortium, University of Oxford, Old Road Campus Research Building, Old Road Campus, Roosevelt Drive, Oxford OX3 7DQ, U.K.

[‡]Target Discovery Institute, University of Oxford, NDM Research Building, Old Road Campus, Roosevelt Drive, Oxford OX3 7FZ, U.K.

[§]Cell Biology Group, Strathclyde Institute of Pharmacy and Biomedical Sciences, University of Strathclyde, Glasgow G4 0RE, U.K.

ABSTRACT: The most potent inhibitor of Sphingosine Kinase 1 (SPHK1) so far identified is PF-543. The crystal structure of SPHK1 in complex with inhibitor PF-543 to 1.8 Å resolution reveals the inhibitor bound in a bent conformation analogous to that expected of a bound sphingosine substrate but with a rotated head group. The structural data presented will aid in the design of SPHK1 and SPHK2 inhibitors with improved properties.

KEYWORDS: SPHK1, PF-543, SPHK2, sphingosine, lipid, S1P
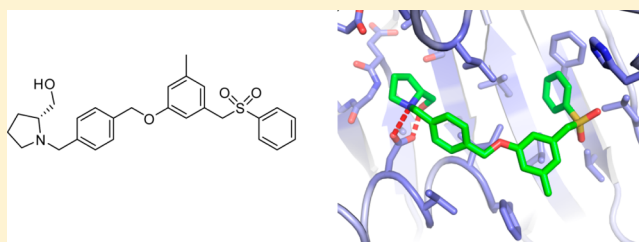
Sphingosine kinases catalyze the conversion of sphingosine to sphingosine-1-phosphate (S1P), the final step of S1P biosynthesis.[1−4] There are two sphingosine kinases: Sphingosine Kinase 1 (SPHK1) is mostly localized to the cytosol while Sphingosine Kinase 2 (SPHK2) is mostly nuclear.[5−7] SPHK2 has 53% sequence identity with SPHK1, but SPHK2 has a large insertion in the lipid binding domain of 134 residues, compared to 18 residues for the equivalent loop in SPHK1, and this insertion contains a significant proportion of proline residues indicating structural disorder. SPHK1 and SPHK2 have some compensatory activities, and while SPHK1 and SPHK2 double knockout mice are embryonically lethal,[8] individual knockouts remain viable,[9] one major reason being that absence of SPHK2 up-regulates SPHK1 expression. Potential individual roles in cell biology of SPHK1 and SPHK2 have been recently reviewed.[10,11] The links between S1P formation and disease are strong, especially in relation to cancer and inflammation.[11−15]

A variety of sphingosine kinase inhibitors have been developed.[16,17] However, most are analogues of sphingosine and show only micromolar affinity. Targeting the S1P pathway has resulted in clinical use of one therapeutic agent, FTY720 (Fingolimod, Gilenya), approved for treatment of relapsing-remitting multiple sclerosis.[18] FTY720 inhibits the action of SPHK1 and SPHK2 in phosphorylating sphingosine[19] and is itself phosphorylated by SPHK2 causing it to act as a functional antagonist of sphingosine-1-phosphate receptor 1 (S1PR1 or S1P1). This is achieved by inducing proteasomal degradation of S1PR1 to create S1PR1 null T-lymphocytes that are unable to egress from lymph nodes into the circulation.[20] To avoid potential issues with lipid analogues, including lack-of-specificity, some non-sphingosine analogue inhibitors have also been developed,[21−24] although the specificity for these is also not well characterized. Recently, use of high-throughput screening and medicinal chemistry optimization allowed development of the non-lipid PF-543 (**1**, Chart 1).[25] A K_i of 4.3 nM and more than 100-fold selectivity

Chart 1. PF-543 Chemical Structure

1, PF-543
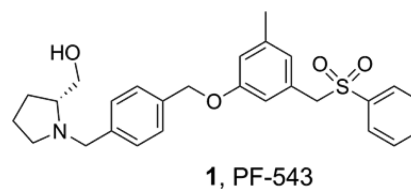
for SPHK1 over SPHK2 were reported.[25] Compound **1** showed no effect on endogenous ceramide levels but reduced S1P levels in 1483 head/neck carcinoma cells.[25]

Structures of SPHK1 were recently reported in complex with inhibitor SKI-II and ADP and in complex with a bound lipid.[26] These structures revealed the expected structural homology of SPHKs to the diacylglycerol kinases, with the lipid bound in a bent conformation in a completely enclosed largely hydrophobic pocket. These structures were used to develop an optimized inhibitor with 20 nM affinity, which was also characterized structurally.[27]

Here, we have determined the crystal structure of SPHK1 with **1**, the most potent SPHK1 inhibitor reported to date. Analysis of the structure suggests ways to design inhibitors with improved SPHK1 or SPHK2 selectivity, as well as ways to take advantage of SPHK features that might allow improved inhibitor selectivity over other enzymes in the ceramide/sphingosine biosynthetic pathway.

Residues 81−449 of SPHK1 isoform 2 (NP_892010.2, NCBI database) were cloned into a baculovirus expression system, which was used to produce SPHK1 protein of high purity suitable for crystallization. This is equivalent to 9−377 of isoform

1 (NP_068807.2) or 1−363 of isoform 3 (NP_001136074.1), with the crystallized construct containing N-terminal residues with no equivalent in isoform 3. The protein was monomeric in solution, showing a single peak on size-exclusion chromatography, and was co-crystallized with **1** and ADP yielding a structure of the SPHK1: **1** complex to 1.8 Å resolution (Figure 1A), the best resolution yet reported for a SPHK1 crystal structure.
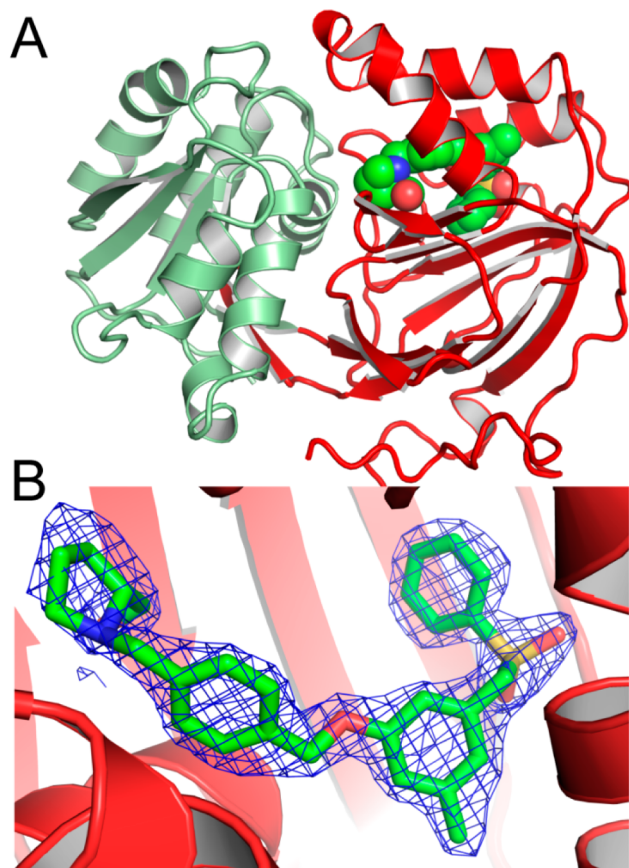

Figure 1. Binding of PF-543 (**1**) to SPHK1. (A) Compound **1** shown as a green spheres model binds in the lipid binding site in the C-terminal domain of SPHK1, shown in red. The N-terminal nucleotide binding domain of SPHK1 is shown in light green. (B) A $2F_0 − F_c$ map is shown contoured at 1.0σ around **1**. The compound was well resolved in the electron density. Only around the pyrrolidine head group was the electron density slightly imperfect, which could perhaps correspond to a small fraction of **1** in a conformation with the head group rotated 180° or to a small proportion of SPHK1 with bound lipid from the Sf9 cells in place of **1** (see text for discussion).

There were two molecules in the crystallographic asymmetric unit. In each, SPHK1 residues 93−449 were resolved in the electron density with the exception of the loop comprising residues 312−317, which was disordered. This is the loop that is greatly extended and predicted to be disordered in SPHK2, so it is not surprising that it is also disordered in SPHK1. Mass spectrometry showed the partial phosphorylation of the protein but no phosphorylation site was obvious in the electron density although the known site of ERK phosphorylation, Ser311 (Ser225 in SPHK1 isoform 3), is poorly ordered, being adjacent to the disordered loop 312−317. Although residues 81−87 from the crystallized sequence are not conserved between SPHK1 isoforms 1, 2, and 3, as this region was not

resolved in the electron density, there is no practical difference in the sequence of the structure compared to those already published,[26] which used isoform 3 (NP_001136074.1).

The structure superimposes with the previous structure of SPHK1:SKI-II:ADP[26] with a root-mean-square deviation (rmsd) of 0.52 Å over 333 Cα atoms. Although ADP was added to the protein used for crystallization, as well as compound **1**, no ADP was visible in the electron density, and the protein loops surrounding the nucleotide binding site have among the highest temperature factors. In the structure of SPHK1:SKI-II:ADP the ADP is also only visible in two out of the six molecules in the asymmetric unit.[26] The inhibitor **1** was, however, clearly resolved in the electron density in both molecules in the asymmetric unit, bound in the completely enclosed lipid binding site in the C-terminal domain of the protein (Figure 1B).

Compound **1** adopts a bent conformation, mimicking the conformation of the lipid observed bound in one of the previous structures of SPHK1 (PDB ID 3VZB)[26] with the terminal phenyl ring occupying a hydrophobic pocket formed by residues including Phe374 and Leucines 347, 354, and 405 (Figure 2).
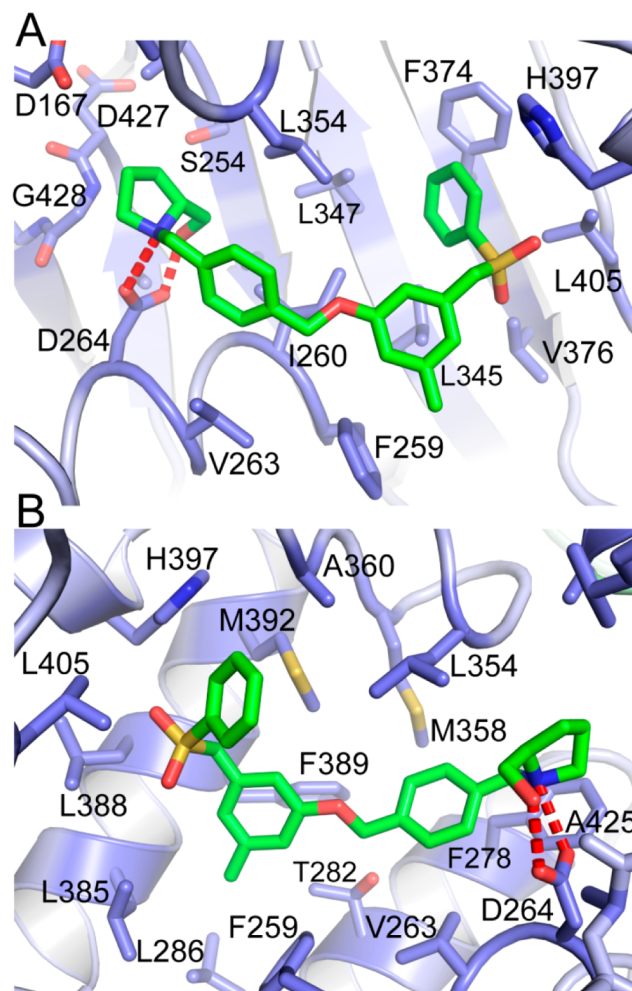

Figure 2. Binding of PF-543 (**1**) to SPHK1 viewed from two opposite directions with **1** shown in green. In each figure the residues in front of **1** have been removed for clarity. Residues are numbered for SPHK1 isoform 2 as crystallized; subtract 72 to get the equivalent residues in isoform 1 or 86 to get the equivalent residues in isoform 3 (as used in the previous structure of SPHK1).

The terminal 1-substituted (R)-2-(hydroxymethyl)-pyrrolidine is bound in the expected position for a lipid head group, adjacent to the binding site for the ATP γ-phosphate. Hydrogen bonds are formed from the pyrrolidine nitrogen and the hydroxyl of 1 to the side-chain of Asp264 (Figure 2). Asp264 is equivalent to mouse SPHK1 Asp177, which was shown to be involved in sphingosine recognition.[28] Modeling suggested that this residue binds the protonated amine of the SPHK1 inhibitor RB-005.[17] The central methyl-substituted aromatic ring of 1 forms favorable edge-on interactions with the side-chains of Phe259 and Phe389 while its methyl substituent packs against Leu385 and Leu286. Unexpectedly, the side-chain of Thr282, one of the few non-hydrophobic residues in the lipid binding site, does not form a hydrogen bond to the ether oxygen of 1.

Compound 1 is reported to be a weak substrate for SPHK1.[25] In order to be phosphorylated, its (R)-2-(hydroxymethyl)-pyrrolidine head group would need to rotate ~180° to bring the primary hydroxyl into a position equivalent to that of the lipid primary hydroxyl in PDB ID 3VZB[26] (Figure 3). The need for
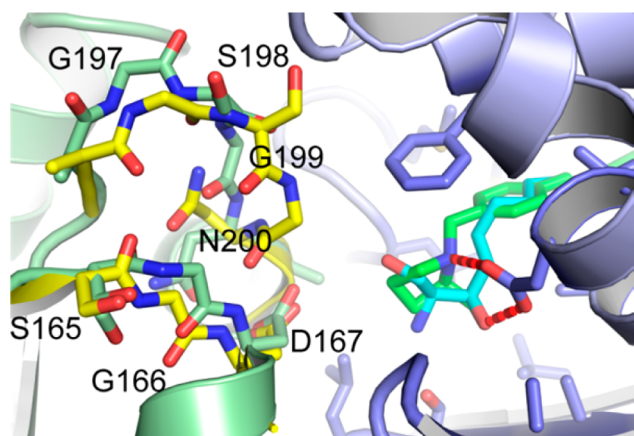

Figure 3. Overlay of the binding PF-543 (1) (in green) and the lipid seen in PDB ID 3VZB (in cyan) to SPHK1 (with N-terminal ATP-binding domain in green and C-terminal lipid-binding domain in blue). The alternative conformation of residues 197−200 in the lipid-bound structure is shown in yellow.

this rotation, which would break the two hydrogen bonds to Asp264, provides a reasonable explanation for the weak substrate activity of 1.

The loop containing residues 197−200 is in a different conformation in each of the two molecules in the asymmetric unit. In chain A 197−200 are different compared to previous structures (Figure 3), being further away from the lipid binding site, while in chain B 197−200 are partially disordered. This loop is expected to be flexible depending on the presence or absence of bound ATP or ADP and may represent an opportunity for inhibitor expansion. Use of the considerable space adjacent to the head group of 1 could allow removal of the substrate activity, as well as optimization of selectivity over all other enzymes in the ceramide/sphingosine biosynthesis pathway.

Currently, research into the biological effects and target potential of the S1P biosynthetic pathway is hampered by the lack of highly potent and selective inhibitors for either SPHK1 or SPHK2. This new structure of SPHK1 in complex with the highest potency SPHK1 inhibitor published to date should aid in the development of inhibitors with improved selectivity and potency. Modeling of the binding of 1 to SPHK2 should aid the development of highly potent and selective SPHK2 inhibitors,

of which none currently exist. SPHK2 has three residue differences in the lipid binding site compared to SPHK1. Phe374 is Cys in SPHK2 (Figure 2A), while Ile260 is Val in SPHK2 and Met358 is Leu. All three of these differences make the binding site larger in SPHK2 compared to SPHK1 suggesting both that inhibitor expansion could create an SPHK2-specific molecule and that it may be difficult to create an SPHK1 inhibitor with no activity at all against SPHK2. The temperature factors of inhibitor 1 in the structure suggest that the terminal phenyl ring that binds against Phe374 may be the tightest bound part of the molecule. Therefore, the substitution of Phe374 for Cys in SPHK2 may be a significant cause of the previously observed ∼132-fold selectivity of 1 for SPHK1 over SPHK2. Optimization of the interactions with Phe374 may aid further improvement in SPHK1 selectivity, while enlargement of the inhibitor to pack against Cys could promote SPHK2 selectivity.

There is potential for introduction of three-dimensional inhibitor functionality to fit the large central part of the lipid-binding pocket, where the methyl-substituted aromatic ring of 1 binds. This is the where the adamantane ring of the SPHK2-selective inhibitor ABC294640[22] would be expected to bind. Given the nonlinear binding shown by 1, a macrocyclic inhibitor might also be possible. Introduction of suitable three-dimensionality might be a way to gain selectivity over other enzymes in the ceramide/sphingosine biosynthetic pathway where such enzymes have linear lipid binding sites.

■ MATERIALS AND METHODS

Cloning. DNA for residues 81−449 of SPHK1 isoform 2 (NM_182965.2) was PCR amplified and subcloned into an in-house pFastBac-based vector pFB-LIC-Bse[29] using ligation-independent cloning. The DNA template for SPHK1 isoform 2 was obtained from the Mammalian Gene Collection (IMAGE Consortium Clone ID 4871343). The resulting construct expressed the desired protein with an N-terminal hexahistidine tag and TEV (tobacco etch virus) protease tag cleavage site (extension MGHHHHHHSSGVDLGTENLYFQ*SM-).

Protein Expression and Purification. The construct DNA was used to prepare recombinant baculovirus, which was used to infect Sf9 cells at a density of 2 million cells/mL in glass conical flasks. The flasks were shaken at 27 °C for 48 h before cells were harvested by centrifugation. The cells were resuspended in Binding Buffer (50 mM Tris·HCl pH 7.8, 200 mM NaCl, 20 mM imidazole, 0.5 mM tris-(2-carboxyethyl)phosphine (TCEP), and protease inhibitor cocktail (Sigma-Aldrich)). The resuspended cells were frozen until further use. For purification the cells were thawed and lysed by sonication on ice. PEI (polyethylenimine) was added to a final concentration of 0.15%, and the cell debris and precipitated DNA were spun down. The supernatant was passed through a gravity column of 5 mL of Ni-Sepharose resin (GE Healthcare). After washing the resin, the protein was eluted with Binding Buffer containing 250 mM imidazole. The N-terminal His tag was removed by addition of TEV (tobacco etch virus) protease overnight at 4 °C, while the protein was dialyzed into GF Buffer (20 mM Tris·HCl pH 7.8, 200 mM NaCl, and 0.5 mM TCEP). The protein was passed through a column of Ni-Sepharose and then concentrated to 5 mL volume and injected onto a S200 16/60 gel filtration column (GE Healthcare) pre-equilibrated into GF Buffer. Fractions containing SPHK1 were pooled and concentrated to 10 mg/mL. Expected molecular weight: 41120.1 Da. Measured molecular weight by electrospray ionization: 41120.2 and 41201.8 Da (1× phosphorylation).

Structure Determination. Crystals were obtained using the sitting drop vapor diffusion method at 4 °C. Crystals grew from a mixture of 100 nL of SPHK1 protein (10 mg/mL with 1 mM PF-543 and 1 mM ADP) and 50 nL of a well solution containing 37.5% MPD, 0. One molar BisTris pH 5.5 and 0.1 M ammonium acetate. Crystals were mounted in nylon loops before freezing in liquid nitrogen. Data was collected at 100 K at the Diamond Synchrotron beamline I02.

The diffraction data was indexed and integrated using XDS[30] and scaled using AIMLESS.[31] The structure was solved by molecular replacement using PHASER[32] and the structure of SPHK1 (PDB ID 3VZB[26]) as the search model. There were two molecules of SPHK1 in the asymmetric unit. The model was built using Coot,[33] refined with REFMAC5,[34] and validated using MOLPROBITY.[35] All structure figures were created using PyMOL (Schrödinger LLC). Data collection statistics can be seen in Table 1.

Table 1. X-ray Data Statistics

space group	$P2_1$
mols in the asymmetric unit	2
unit cell a, b, c (Å), β (deg)	86.6, 60.5, 89.6, 107.2
resolution range (Å)^a	43.63−1.80 (1.83−1.80)
unique observations^a	82290 (4505)
average multiplicity^a	6.6 (6.4)
completeness (%)^a	100.0 (100.0)
R_{merge}^{a}	0.11 (0.96)
mean $(I)/\sigma(I)$^{a}	11.0 (1.8)
mean CC(1/2)^a	0.998 (0.652)
R-value, R_{free} (%)	18.2, 21.0
rmsd from ideal bond lengths (Å)/angles (deg)	0.013/1.49

^{a}Values within parentheses refer to the highest resolution shell.

ASSOCIATED CONTENT

Accession Codes

The structure coordinates have been deposited in the Protein Data Bank, ID 4V24.

AUTHOR INFORMATION

Corresponding Author

*E-mail: jon.elkins@sgc.ox.ac.uk.

Author Contributions

All authors have given approval to the final version of the manuscript.

Notes

The authors declare no competing financial interest.

ABBREVIATIONS

SPHK1, sphingosine kinase 1; SPHK2, sphingosine kinase 2; S1P, sphingosine-1-phosphate

REFERENCES

(1) Kohama, T.; Olivera, A.; Edsall, L.; Nagiec, M. M.; Dickson, R.; Spiegel, S. Molecular Cloning and Functional Characterization of Murine Sphingosine Kinase. *J. Biol. Chem.* **1998**, *273*, 23722−23728.

(2) Olivera, A.; Kohama, T.; Tu, Z.; Milstien, S.; Spiegel, S. Purification and Characterization of Rat Kidney Sphingosine Kinase. *J. Biol. Chem.* **1998**, *273*, 12576−12583.

(3) Liu, H.; Sugiura, M.; Nava, V. E.; Edsall, L. C.; Kono, K.; Poulton, S.; Milstien, S.; Kohama, T.; Spiegel, S. Molecular Cloning and Functional Characterization of a Novel Mammalian Sphingosine Kinase Type 2 Isoform. *J. Biol. Chem.* **2000**, *275*, 19513−19520.

(4) Pitson, S. M.; D'andrea, R. J.; Vandeleur, L.; Moretti, P. A.; Xia, P.; Gamble, J. R.; Vadas, M. A.; Wattenberg, B. W. Human Sphingosine Kinase: Purification, Molecular Cloning and Characterization of the Native and Recombinant Enzymes. *Biochem. J.* **2000**, *350* (Pt 2), 429−441.

(5) Ding, G.; Sonoda, H.; Yu, H.; Kajimoto, T.; Goparaju, S. K.; Jahangeer, S.; Okada, T.; Nakamura, S. Protein Kinase D-Mediated Phosphorylation and Nuclear Export of Sphingosine Kinase 2. *J. Biol. Chem.* **2007**, *282*, 27493−27502.

(6) Hait, N. C.; Allegood, J.; Maceyka, M.; Strub, G. M.; Harikumar, K. B.; Singh, S. K.; Luo, C.; Marmorstein, R.; Kordula, T.; Milstien, S.; Spiegel, S. Regulation of Histone Acetylation in the Nucleus by Sphingosine-1-Phosphate. *Science* **2009**, *325*, 1254−1257.

(7) Maceyka, M.; Sankala, H.; Hait, N. C.; Le Stunff, H.; Liu, H.; Toman, R.; Collier, C.; Zhang, M.; Satin, L. S.; Merrill, A. H.; Milstien, S.; Spiegel, S. SphK1 and SphK2, Sphingosine Kinase Isoenzymes with Opposing Functions in Sphingolipid Metabolism. *J. Biol. Chem.* **2005**, *280*, 37118−37129.

(8) Mizugishi, K.; Yamashita, T.; Olivera, A.; Miller, G. F.; Spiegel, S.; Proia, R. L. Essential Role for Sphingosine Kinases in Neural and Vascular Development. *Mol. Cell. Biol.* **2005**, *25*, 11113−11121.

(9) Allende, M. L.; Sasaki, T.; Kawai, H.; Olivera, A.; Mi, Y.; van Echten-Deckert, G.; Hajdu, R.; Rosenbach, M.; Keohane, C. A.; Mandala, S.; Spiegel, S.; Proia, R. L. Mice Deficient in Sphingosine Kinase 1 Are Rendered Lymphopenic by FTY720. *J. Biol. Chem.* **2004**, *279*, 52487−52492.

(10) Maceyka, M.; Spiegel, S. Sphingolipid Metabolites in Inflammatory Disease. *Nature* **2014**, *510*, 58−67.

(11) Kunkel, G. T.; Maceyka, M.; Milstien, S.; Spiegel, S. Targeting the Sphingosine-1-Phosphate Axis in Cancer, Inflammation and Beyond. *Nat. Rev. Drug Discovery* **2013**, *12*, 688−702.

(12) Liang, J.; Nagahashi, M.; Kim, E. Y.; Harikumar, K. B.; Yamada, A.; Huang, W.-C.; Hait, N. C.; Allegood, J. C.; Price, M. M.; Avni, D.; Takabe, K.; Kordula, T.; Milstien, S.; Spiegel, S. Sphingosine-1-Phosphate Links Persistent STAT3 Activation, Chronic Intestinal Inflammation, and Development of Colitis-Associated Cancer. *Cancer Cell* **2013**, *23*, 107−120.

(13) Pyne, N. J.; Pyne, S. Sphingosine 1-Phosphate and Cancer. *Nat. Rev. Cancer* **2010**, *10*, 489−503.

(14) Lai, W.-Q.; Wong, W. S. F.; Leung, B. P. Sphingosine Kinase and Sphingosine 1-Phosphate in Asthma. *Biosci. Rep.* **2011**, *31*, 145−150.

(15) Pyne, N. J.; Pyne, S. Sphingosine 1-Phosphate Is a Missing Link between Chronic Inflammation and Colon Cancer. *Cancer Cell* **2013**, *23*, 5−7.

(16) Plano, D.; Amin, S.; Sharma, A. K. Importance of Sphingosine Kinase (SphK) as a Target in Developing Cancer Therapeutics and Recent Developments in the Synthesis of Novel SphK Inhibitors. *J. Med. Chem.* **2014**, *57*, 5509−5524.

(17) Baek, D. J.; MacRitchie, N.; Anthony, N. G.; Mackay, S. P.; Pyne, S.; Pyne, N. J.; Bittman, R. Structure-Activity Relationships and Molecular Modeling of Sphingosine Kinase Inhibitors. *J. Med. Chem.* **2013**, *56*, 9310−9327.

(18) Sanford, M. Fingolimod: A Review of Its Use in Relapsing-Remitting Multiple Sclerosis. *CNS Drugs* **2011**, *25*, 673−698.

(19) Tonelli, F.; Lim, K. G.; Loveridge, C.; Long, J.; Pitson, S. M.; Tigyi, G.; Bittman, R.; Pyne, S.; Pyne, N. J. FTY720 and (S)-FTY720 Vinylphosphonate Inhibit Sphingosine Kinase 1 and Promote Its Proteasomal Degradation in Human Pulmonary Artery Smooth Muscle, Breast Cancer and Androgen-Independent Prostate Cancer Cells. *Cell. Signalling* **2010**, *22*, 1536−1542.

(20) Chun, J.; Brinkmann, V. A Mechanistically Novel, First Oral Therapy for Multiple Sclerosis: The Development of Fingolimod (FTY720, Gilenya). *Discovery Med.* **2011**, *12*, 213−228.

(21) French, K. J.; Schrecengost, R. S.; Lee, B. D.; Zhuang, Y.; Smith, S. N.; Eberly, J. L.; Yun, J. K.; Smith, C. D. Discovery and Evaluation of Inhibitors of Human Sphingosine Kinase. *Cancer Res.* **2003**, *63*, 5962−5969.

(22) French, K. J.; Zhuang, Y.; Maines, L. W.; Gao, P.; Wang, W.; Beljanski, V.; Upson, J. J.; Green, C. L.; Keller, S. N.; Smith, C. D. Pharmacology and Antitumor Activity of ABC294640, a Selective Inhibitor of Sphingosine Kinase-2. *J. Pharm. Exp. Ther.* **2010**, *333*, 129−139.

(23) Sharma, A. K.; Sk, U. H.; Gimbor, M. A.; Hengst, J. A.; Wang, X.; Yun, J.; Amin, S. Synthesis and Bioactivity of Sphingosine Kinase Inhibitors and Their Novel Aspirinyl Conjugated Analogs. *Eur. J. Med. Chem.* **2010**, *45*, 4149−4156.

(24) Hengst, J. A.; Wang, X.; Sk, U. H.; Sharma, A. K.; Amin, S.; Yun, J. K. Development of a Sphingosine Kinase 1 Specific Small-Molecule Inhibitor. *Bioorg. Med. Chem. Lett.* **2010**, *20*, 7498−7502.

(25) Schnute, M. E.; McReynolds, M. D.; Kasten, T.; Yates, M.; Jerome, G.; Rains, J. W.; Hall, T.; Chrencik, J.; Kraus, M.; Cronin, C. N.; Saabye, M.; Highkin, M. K.; Broadus, R.; Ogawa, S.; Cukyne, K.; Zawadzke, L. E.; Peterkin, V.; Iyanar, K.; Scholten, J. A.; Wendling, J.; Fujiwara, H.; Nemirovskiy, O.; Wittwer, A. J.; Nagiec, M. M. Modulation of Cellular S1P Levels with a Novel, Potent and Specific Inhibitor of Sphingosine Kinase-1. *Biochem. J.* **2012**, *444*, 79−88.

(26) Wang, Z.; Min, X.; Xiao, S.-H.; Johnstone, S.; Romanow, W.; Meininger, D.; Xu, H.; Liu, J.; Dai, J.; An, S.; Thibault, S.; Walker, N. Molecular Basis of Sphingosine Kinase 1 Substrate Recognition and Catalysis. *Structure* **2013**, *21*, 798−809.

(27) Gustin, D. J.; Li, Y.; Brown, M. L.; Min, X.; Schmitt, M. J.; Wanska, M.; Wang, X.; Connors, R.; Johnstone, S.; Cardozo, M.; Cheng, A. C.; Jeffries, S.; Franks, B.; Li, S.; Shen, S.; Wong, M.; Wesche, H.; Xu, G.; Carlson, T. J.; Plant, M.; Morgenstern, K.; Rex, K.; Schmitt, J.; Coxon, A.; Walker, N.; Kayser, F.; Wang, Z. Structure Guided Design of a Series of Sphingosine Kinase (SphK) Inhibitors. *Bioorg. Med. Chem. Lett.* **2013**, *23*, 4608−4616.

(28) Yokota, S.; Taniguchi, Y.; Kihara, A.; Mitsutake, S.; Igarashi, Y. Asp177 in C4 Domain of Mouse Sphingosine Kinase 1a Is Important for the Sphingosine Recognition. *FEBS Lett.* **2004**, *578*, 106−110.

(29) Savitsky, P.; Bray, J.; Cooper, C. D. O.; Marsden, B. D.; Mahajan, P.; Burgess-Brown, N. A.; Gileadi, O. High-Throughput Production of Human Proteins for Crystallization: The SGC Experience. *J. Struct. Biol.* **2010**, *172*, 3−13.

(30) Kabsch, W. XDS. *Acta Crystallogr.* **2010**, *D66*, 125−132.

(31) Winn, M. D.; Ballard, C. C.; Cowtan, K. D.; Dodson, E. J.; Emsley, P.; Evans, P. R.; Keegan, R. M.; Krissinel, E. B.; Leslie, A. G. W.; McCoy, A.; McNicholas, S. J.; Murshudov, G. N.; Pannu, N. S.; Potterton, E. A.; Powell, H. R.; Read, R. J.; Vagin, A.; Wilson, K. S. Overview of the CCP4 Suite and Current Developments. *Acta Crystallogr.* **2011**, *D67*, 235−242.

(32) McCoy, A. J.; Grosse-Kunstleve, R. W.; Adams, P. D.; Winn, M. D.; Storoni, L. C.; Read, R. J. Phaser Crystallographic Software. *J. Appl. Crystallogr.* **2007**, *40*, 658−674.

(33) Emsley, P.; Lohkamp, B.; Scott, W. G.; Cowtan, K. Features and Development of Coot. *Acta Crystallogr.* **2010**, *D66*, 486−501.

(34) Murshudov, G. N.; Skubák, P.; Lebedev, A. A.; Pannu, N. S.; Steiner, R. A.; Nicholls, R. A.; Winn, M. D.; Long, F.; Vagin, A. A. REFMAC5 for the Refinement of Macromolecular Crystal Structures. *Acta Crystallogr.* **2011**, *D67*, 355−367.

(35) Chen, V. B.; Arendall, W. B.; Headd, J. J.; Keedy, D. A.; Immormino, R. M.; Kapral, G. J.; Murray, L. W.; Richardson, J. S.; Richardson, D. C. MolProbity: All-Atom Structure Validation for Macromolecular Crystallography. *Acta Crystallogr.* **2010**, *D66*, 12−21.